3B3-4

Effect of Photoelectrons on the Impedance of Electric Field Antenna onboard Spacecraft

#Yohei Miyake[1], Hideyuki Usui[1], Hirotsugu Kojima[1], Yoshiharu Omura[1], Hiroshi Matsumoto[1]

[1] Research Institute for Sustainable Humanosphere (RISH), Kyoto University
Gokasho, Uji, Kyoto 611-0011, JAPAN, y-miyake@rish.kyoto-u.ac.jp

1. Introduction

Many scientific spacecrafts are equipped with electric field antennas for the plasma wave investigations, which are basically dipole antennas. The plasma wave investigations should cover a large frequency range, from the DC range to that above the electron plasma or cyclotron frequencies. This means that the antenna characteristics can be influenced by the frequency-dependent nature of surrounding space plasma. For this reason, although elementary instruments such as the dipole antennas are used, the complex antenna characteristics (e.g., impedance) have not been sufficiently understood and have to be investigated for the wave data calibration as well as in the antenna design for space missions. One of the important points to be considered is the inhomogeneous plasma distribution around the antenna. In many previous works (e.g., [1]), antenna is assumed to be an ideal thin conductive wire, totally transparent to the fluid plasma medium. However, antenna surface is a solid body and plasma particles which impinge the surface are absorbed at the surface and contribute to the charging, creating an ion sheath around the antenna surface.

In the current study, we consider the plasma dynamics and applied the PIC (Particle-In-Cell) method to the conventional FDTD field solving simulation for the antenna analysis. By using the PIC modeling for plasma simulations, we can self-consistently consider the plasma kinetic effects such as sheath formation. This enables us to naturally include the effects of the inhomogeneous plasma environment. We particularly modeled a situation of photoelectron emission from the antenna surface and investigated the dependence of antenna impedance on the photoelectron density in the frequency domain.

2. Simulation Model

By modifying the three-dimensional electromagnetic (EM) PIC simulation code called KEMPO [2], we developed an antenna simulator. We show the simulation model in Fig. 1. Spacecraft is modeled as a solid body made of conducting surface. We set a spacecraft body and two mono pole antennas in the center, each of which is attached to the top and bottom surfaces of the spacecraft respectively. To obtain the equipotential solution for the conducting spacecraft surface including antennas we redistribute the surface charge by using Capacity Matrix Method [3] and correct the electrostatic field by solving Poisson's equation in consideration with the modified surface charge. The joints between the antennas and the spacecraft are assumed to be electrically insulated.

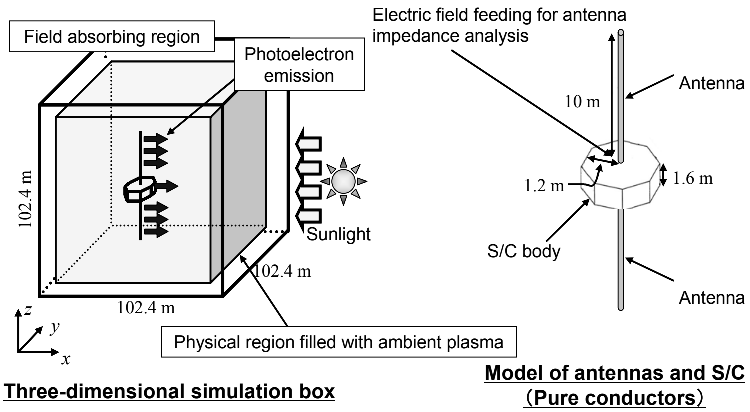

Figure 1: Three-dimensional Simulation Model for Antenna Analysis in the Photoelectron Environment.

To simulate the photoelectron emission from the spacecraft surface, we use the standard algorithm for the electron injection from the conducting bodies [4]. By using the net charge on the surfaces and the charge of the background plasma, we solve Poisson's equation to obtain the potential values and the electric field at each grid point as stated above. Then the floating potential of the antennas and the spacecraft body can be obtained in the self-consistent manner. In the current study, we combined two simulation runs for the antenna analysis. First we perform an ES (electrostatic) simulation which focuses on the creation of plasma environment around the spacecraft. After obtaining the plasma environment around the spacecraft and antenna with the above ES simulation, we move to the EM (electromagnetic) simulation for antenna analysis. To obtain the input impedance of the antenna we adopted the Delta-gap feeding method. In this method, we treat the antenna as a transmitting one and provide voltage of a Gaussian-type pulse at the power feeding point. The antenna input impedance is calculated as the ratio of the voltage to the current.

Table 1: Parameters used in the Simulation.

	Parameters	Value
Background electron	Density	$5.0\times10^{6}\,m^{-3}$
	Temperature	$5.0\times10^{5}\,K$
	Debye length	21.8 m
Photoelectron	Photoelectron current density I_n (when incident angle θ : I_θ)	$5.0\times10^{-5}\,Am^{-2}$ $I_\theta=\cos\theta\times I_n$
	Temperature (Energy)	$1.86\times10^{4}\,K$ (1.6 eV)
	Energy spectrum	Maxwellian

3. Simulation Results

We examined a general case to see how the antenna characteristics are modified by photoemissions emitted from spacecraft. We consider a situation that a spacecraft is immersed in the magnetospheric plasma, and the sun illuminates the spacecraft body from the direction perpendicular to the antennas. As shown in Table 1, the realistic parameters for the photo- and background-plasma electrons in magnetosheath are used in the simulation. The temperature of the photoelectron is much smaller than that of the background electron. Meanwhile, the density of the photoelectron is much larger than that of the background electron.

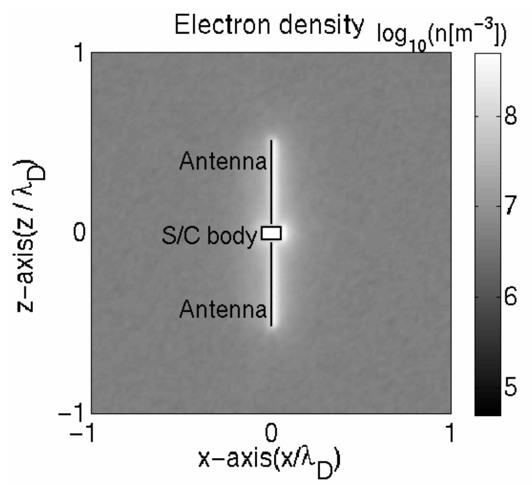

Figure 2: Contour map of electron density around the spacecraft and antenna.

By using these parameters, we performed ES simulation for the analysis of the plasma environment in the vicinity of the spacecraft. We conducted the simulation with sufficient time steps, so that the floating potentials reach to an equilibrium state. The obtained floating potentials are 6.1 V and 11.7 V for the antenna and spacecraft bodies, respectively. On the other hand, by using an analytical formula for the floating potential of a conductor with simple configuration, we obtain ~4 V for the spacecraft body. Because we neglect the presence of plural conducting bodies in the analytical estimation, there is difference between the simulation and analytical results. However, it is confirmed that the correct order of the floating potential is obtained by the present simulation.

Fig. 2 shows a contour plot of electron density around the antennas and spacecraft body. The electron density is measured in the *x-z* plane, which slices the center of the antennas and spacecraft. In the present analysis, we simulated a situation that photoelectrons are emitted from both upper and lower antennas and the spacecraft body to the positive direction of *x*-axis. As shown in Fig. 2, a photoelectron cloud with high electron density is created around the antennas and spacecraft body. Around the spacecraft body, the photoelectron cloud mainly locates only in front of the sunlit surfaces, while it distributes around the antennas so that the electron dense region surrounds the whole surfaces. It indicates that there are photoelectrons which move to the back of antennas because the radial dimension of the antennas is smaller than the characteristic length of photoelectrons. Around the sunlit antennas, the electron density is approximately 1.5×10^8 m^{-3}. At the spacecraft surfaces, we confirmed the same order of the electron density.

By using the plasma environment which is self-consistently obtained with the ES simulation described above, we conducted EM simulation for the analysis of the antenna impedance. Fig. 3 shows the real and imaginary parts of the antenna impedance as a function of frequency obtained in the EM simulation. The solid and dashed lines correspond to the cases of the photoelectron environment and free space, respectively. The impedance modification by the photoelectron environment is found at the low frequency range. The resistance increases as the frequency approaches to zero, and the absolute value of the reactance becomes smaller in comparison with the free space case at the low-frequency range. The notable feature is that the discrepancy between the cases of the photoelectron environment and free space become larger, as the frequency approaches to zero. In contrast, the high-frequency impedance shows little difference between the cases of the photoelectron environment and free space.

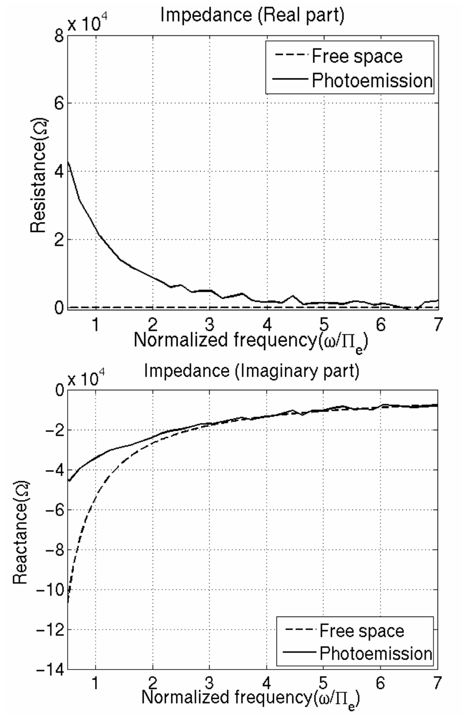

Figure 3: Antenna resistance (upper) and reactance (lower) obtained by the EM-PIC simulations.

4. Equivalent Circuit of Antenna Impedance

We interpret this modification in the aspect of equivalent electric circuit of the antenna impedance. As previously stated, the antenna impedance in free space has a pure capacitance C_0. In plasma, on the other hand, the finite conductivity of the antenna-surrounding medium should be considered. In the aspect of electric circuit, a resistance R_L with a finite value that controls the plasma conduction current flowing between the antennas and the spacecraft body can be assumed and is placed in parallel to the capacitance C_0. The resistance R and reactance X in terms of a serial impedance for this parallel circuit are given as $R_L/(1+(\omega C_0 R_L)^2)$ and $-\omega C_0 R_L^2/(1+(\omega C_0 R_L)^2)$, respectively. By using these formulae, we plot the real and imaginary parts of the impedance for this equivalent circuit in Fig. 4. In Fig. 4, we plot several curves which correspond to the different values of R_L, while the value of C_0 is fixed for each curve. The dashed line represents the impedance in free space (R_L=0). As clearly shown, the resistance gradually increases, and the absolute value of the reactance tends to zero as frequency approaches to zero. This tendency of the impedance modification qualitatively agrees with the impedance profile obtained by the PIC simulations. In addition, we performed several simulation runs with different parameters of photoelectron flux and confirmed that the large photoelectron density around the antenna leads to the small value of the resistance R_L.

The impedance modification as observed in the present analysis was also reported by in-flight measurements of the antenna impedance by the GEOTAIL spacecraft [5]. On the other hand, the effects of conduction current were not included because of its complexity in the formulation in the previous theoretical studies of antenna impedance. The present simulation can handle the effect of the electron conduction current induced by actual motion of photoelectrons impinging the solid surfaces of the antennas and spacecraft body. The impedance modification by the effects of electron conduction current can be observed due to the practical modeling of the antenna-plasma interactions. By the analytical formulation of R_L in a simple situation, the value of R_L is known to be much affected by the total and photoelectron-emitting area of the conducting surfaces. In the present simulation model, due to the lack of the computational resources, the radius of the antenna and the area of the antenna surfaces are not modeled with sufficient spatial resolution. Although, we have to improve the antenna and spacecraft model more realistically in order to evaluate the value in a specific real situation, the simulation code is confirmed to be effective for the quantitative analysis in the complex plasma environment caused by spacecraft-plasma interactions.

5. Summary

We established the basic method for antenna analysis in space plasma by using the three-dimensional PIC simulations. In the present study, we particularly examined the antenna characteristics in the photoelectron environment. By performing ES simulations, we confirmed that photoelectron cloud and ion sheath are created around the sunlit and sunless antenna, respectively. For such a non-uniform plasma environment, numerical simulation is almost only method to calculate the antenna impedance. By using the plasma environment obtained in the ES simulations, we performed EM simulations for the antenna analysis and calculated the antenna impedance as a function of frequency. We found that impedances in photoemission cases are very different from its free-space value in low frequency region. By using a simple equivalent circuit, we analyzed the signature of the antenna impedance and found that a resistance R_L, which corresponds to the electron conductivity at the photoelectron cloud, can be additionally attached in parallel to the antenna capacitance C_0 in the circuit. The additional resistance can play an important role to modify both resistance and reactance in the low frequency region. Since the additional resistance depends on the photoelectron density as well as the configuration of spacecraft and antenna, it is generally difficult to evaluate the value quantitatively. To do this, we need to perform numerical simulations as done in the current study for each specific case after the further improvement of the spacecraft and antenna model.

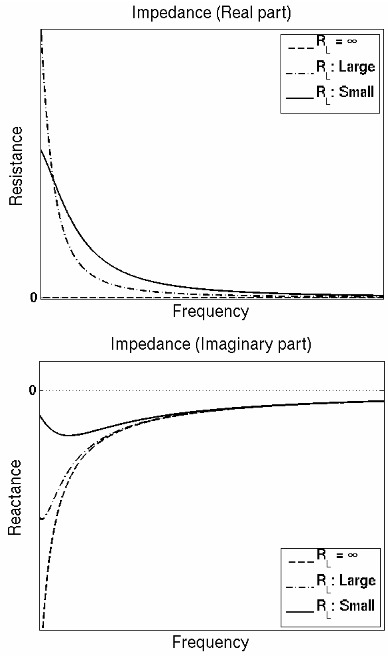

Figure 4: Schematic illustration of dependence of antenna impedance on the additional resistance R_L.

Acknowledgments

Computation in the present study was performed with the KDK system of Research Institute for Sustainable Humanosphere (RISH) at Kyoto University as a collaborative research project. The work was supported by Grant-in-Aid for Research Fellows of the Japan Society for the Promotion of Science (JSPS).

References

[1] K. G. Balmain, “The impedance of a short dipole antenna in a magnetoplasma,” IEEE Trans. Antennas Propag., vol. AP-12, pp. 605–617, 1964.
[2] Y. Omura, and H. Matsumoto, “KEMPO1: Technical guide to one-dimensional electromagnetic particle code,” in Computer Space Plasma Physics: Simulation Techniques and Software, H. Matsumoto and Y. Omura, Terra Scientific, Tokyo, Japan, pp. 21–65, 1933.
[3] R. W. Hockney, and J. W. Eastwood, Computer Simulation Using Particles, McGraw-Hill, New York, 1981.
[4] C. K. Birdsall, and A. B. Langdon, Plasma Physics Via Computer Simulation, McGraw-Hill, New York, 1985.
[5] M. Tsutsui, I. Nagano, H. Kojima, K. Hashimoto, H. Matsumoto, S.Yagitani, and T. Okada, “Measurements and analysis of antenna impedance aboard the Geotail spacecraft,” Radio Sci., vol. 32, pp.1101-1126, 1977.